Resolving high-speed colloidal dynamics beyond detector response time via two pulse speckle contrast correlation

Sooheyong Lee,[1,5] Wonhyuk Jo,[2] Haeng Sub Wi,[1] C. Gutt,[3] and Geun Woo Lee[1,4,*]

[1] *Korea Research Institute of Standards and Science, Daejeon 305-600, South Korea*
[2] *Department of Physics, Soongsil University, Seoul 156-743, South Korea*
[3] *Department Physik, Universität Siegen, Siegen 57068, Germany*
[4] *Department of Science of Measurement, University of Science and Technology, Daejeon, 305-333, South Korea*
[5] *sooheyong@gmail.com*
[*] *gwlee@kriss.re.kr*

Abstract: We report an alternate light scattering approach to measure intermediate scattering function and structures of colloidal suspension by using two-pulse speckle contrast correlation analysis. By systematically controlling time-delays between two laser pulses incident on the sample, we are able to monitor transient evolution of coherent diffraction pattern, from which particle dynamics at different length and time scales are obtained simultaneously. Our result demonstrates the feasibility of utilizing a megapixel detector to achieve sufficient data statistics in a short amount of time while enabling microsecond time-resolution. Ultimately, this method provides means to measure high-speed dynamics well beyond the time response limit of a large area two-dimensional (2D) detector.

OCIS codes: (030.0030) Coherence and statistical optics; (140.2600) Free-electron lasers (FELs); (300.6480) Spectroscopy, speckle.

References and links

1. H. Z. Cummins and E. R. Pike, *Photon Correlation and Light-Beating Spectroscopy* (Plenum Press, N.Y., 1974).
2. B. J. Berne and R. Pecora, *Dynamic Light Scattering: With Applications to Chemistry, Biology, and Physics* (Courier Dover Publications, N.Y., 2000).
3. W. Brown, *Dynamic Light Scattering: The Method and Some Applications* (Claredon Press, Oxford, 1993).
4. D. Pine, D. Weitz, P. Chaikin, and E. Herbolzheimer, "Diffusing wave spectroscopy," Phys. Rev. Lett. **60**, 1134–1137 (1988).
5. M. S. Amin, Y. Park, N. Lue, R. R. Dasari, K. Badizadegan, M. S. Feld, and G. Popescu, "Microrheology of red blood cell membranes using dynamic scattering microscopy," Opt. Express **15**, 17001–17009 (2007).
6. H. C. van de Hulst, *Light Scattering of Small Particles* (Wiley, New York, 1981).
7. M. Kerker, *The Scattering of Light and Other Electromagnetic Radiation* (Academic Press, New York, 1969).
8. C. . F. . Bohren and D. . R. . Huffman, *Absorption and Scattering of Light by Small Particles* (Wiley-Interscience, New York, 1983).
9. J. G. H. Joosten, J. L. McCarthy, and P. N. Pusey, "Dynamic and static light scattering by aqueous polyacrylamide gels," Macromolecules **24**, 6690–6699 (1991).
10. G. F. C., P. Stepanek, S. Vanessa, J. Eliezer, J. Alessandro, and G. Cristiano, "Light scattering evidence of selective protein fouling on biocompatible block copolymer micelles," Nanoscale **4**, 4504–4514 (2012).
11. P. Emma, R. Akre, J. Arthur, R. Bionta, C. Bostedt, J. Bozek, A. Brachmann, P. Bucksbaum, R. Coffee, F.-J. Decker, Y. Ding, D. Dowell, S. Edstrom, A. Fisher, J. Frisch, S. Gilevich, J. Hastings, G. Hays, P. Hering, Z. Huang, R. Iverson, H. Loos, M. Messerschmidt, A. Miahnahri, S. Moeller, H.-D. Nuhn, G. Pile, D. Ratner,

#216973 - $15.00 USD Received 14 Jul 2014; revised 14 Aug 2014; accepted 14 Aug 2014; published 28 Aug 2014

J. Rzepiela, D. Schultz, T. Smith, P. Stefan, H. Tompkins, J. Turner, J. Welch, W. White, J. Wu, G. Yocky, and J. Galayda, "First lasing and operation of an ångstrom-wavelength free-electron laser," Nat. Photonics **4**, 589–591 (2010).
12. T. Shintake, H. Tanaka, T. Hara, T. Tanaka, K. Togawa, M. Yabashi, Y. Otake, Y. Asano, T. Bizen, T. Fukui, S. Goto, A. Higashiya, T. Hirono, N. Hosoda, T. Inagaki, S. Inoue, M. Ishii, Y. Kim, H. Kimura, M. Kitamura, T. Kobayashi, H. Maesaka, T. Masuda, S. Matsui, T. Matsushita, X. Marchal, M. Nagasono, H. Ohashi, T. Ohata, T. Ohshima, K. Onoe, K. Shirasawa, T. Takagi, S. Takahashi, M. Takeuchi, K. Tamasaku, R. Tanaka, Y. Tanaka, T. Tanikawa, T. Togashi, S. Wu, A. Yamashita, K. Yanagida, C. Zhang, H. Kitamura, and T. Ishikawa, "A compact free-electron laser for generating coherent radiation in the extreme ultraviolet region," Nat. Photonics **2**, 555–559 (2009).
13. P. Wochner, C. Gutt, T. Autenrieth, T. Demmer, V. Bugaev, A. D. Ortiz, A. Duri, F. Zontone, G. Grübel, and H. Dosch, "X-ray cross correlation analysis uncovers hidden local symmetries in disordered matter," Proc. Natl. Acad. Sci. U.S.A. **106**, 11511–11514 (2009).
14. B. Pedrini, A. Menzel, M. Guizar-Sicairos, V. A. Guzenko, S. Gorelick, C. David, B. D. Patterson, and R. Abela, "Two-dimensional structure from random multiparticle x-ray scattering images using cross-correlations," Nat. Commun. **4**, 1647 (2013).
15. L. Cipelletti and D. Weitz, "Ultralow-angle dynamic light scattering with a charge coupled device camera based multispeckle, multitau correlator," Rev. sci. instrum. **70**, 3214–3221 (1999).
16. R. Bandyopadhyay, A. S. Gittings, S. S. Suh, P. K. Dixon, and D. J. Durianc, "Speckle-visibility spectroscopy: A tool to study time-varying dynamics," Rev. sci. instrum. **76**, 093110 (2005).
17. P. Dixon and D. Durian, "Speckle Visibility Spectroscopy and Variable Granular Fluidization," Phys. Rev. Lett. **90**, 184302 (2003)
18. Ashwin B. Parthasarathy, W. James Tom, Ashwini Gopal, Xiaojing Zhang, and Andrew K. Dunn, "Robust flow measurement with multi-exposure speckle imaging," Opt. Express **16**, 1975-1989 (2008)
19. C. Gutt, L.-M. Stadler, A. Duri, T. Autenrieth, O. Leupold, Y. Chushkin, and G. Grübel, "Measuring temporal speckle correlations at ultrafast x-ray sources," Opt. Express **17**, 55–61 (2009).
20. Sidhartha S. Jena, Hiren M. Joshi, K.P.V. Sabareesh, B.V.R. Tata, and T.S. Rao, "Dynamics of Deinococcus radiodurans under controlled growth conditions," Biophys J. **91**, 2699–2707 (2006).
21. E. Tamborini and L. Cipelletti, "Multiangle static and dynamic light scattering in the intermediate scattering angle range," Rev. Sci. Instrum. **83**, 093106 (2012).
22. G. Grübel, A. Madsen, and A. Robert, "X-ray photon correlation spectroscopy (XPCS)," in "Soft Matter Characterization," R. Borsali and R. Pecora, eds. (Springer-Verlag, New York, N.Y., 2008), chap. 18, pp. 961–963.
23. J.C. Dainty, "The statistics of speckle patterns," in "Progress in optics," E. Wolf, eds. (North-Holland, 1976), pp. 20.
24. http://www.originlab.com/doc/Origin-Help/NLFit-Algorithm
25. Alfred B. Leung, Kwang I. Suh, and Rafat R. Ansari, "Particle-size and velocity measurements in flowing conditions using dynamic light scattering," Appl. Opt. **34**, 2186–2190 (2006).
26. S. Lee, W. Roseker, C. Gutt, Z. Huang, Y. Ding, G. Grübel, and A. Robert, "High wavevector temporal speckle correlations at the linac coherent light source," Opt. Express **20**, 9790–9800 (2012).
27. S. O. Hruszkewycz, M. Sutton, P. H. Fuoss, B. Adams, S. Rosenkranz, K. F. L. Jr., W. Roseker, D. Fritz, M. Cammarata, D. Zhu, S. Lee, H. Lemke, C. Gutt, A. Robert, G. Grübel, and G. B. Stephenson, "High contrast x-ray speckle from atomic-scale order in liquids and glasses," Phys. Rev. Lett. **109**, 185502 (2012).

1. Introduction

A capability to probe structures and dynamics on small length and respective time-scales holds important merit in a broad spectrum of communities ranging from biology to chemistry and physics as well as providing direct applications in biophysical and pharmaceutical industries. In these fields, light scattering methods such as dynamical light scattering (DLS) [1–5] and static light scattering (SLS) [6–10] have provided indispensable means to characterize various samples such as proteins, molecules, polymers and nano-particles. One of the key properties of DLS is utilizing coherent optical beam to illuminate small objects such as particles in solution, which results in a coherent scattering pattern known as *speckle*. The random movements such as a Brownian motion of the subjected particles shift the relative phases of the scattered fields and induce temporal variation in the speckle patterns. A high-speed point detector such as an avalanche photodiode can be used to measure the intensity fluctuation. However the conventional DLS measurement, which is performed at a fixed detector angle, does not allow simultaneous measurements of angular dependence of the scattered signals. On the other hand, SLS

#216973 - $15.00 USD Received 14 Jul 2014; revised 14 Aug 2014; accepted 14 Aug 2014; published 28 Aug 2014

probes structures of a sample by measuring the time-averaged scattered intensity as a function of wavevector to provide dimensional information such as form and structure factors. Ideally, elaborate studies on inter-particle interactions such as aggregations, structural relaxation and diffusion dynamics require access to both the fast intensity fluctuation and scattered intensity distribution. For instance with a recent emergence of coherent x-ray sources [11, 12], significant effort has been made to deduce geometrical and dynamical information from amorphous systems or randomly oriented objects with various shapes and size by analyzing spatial fluctuation of speckle patterns [13, 14]. While so far various schemes such as using a CCD camera to capture successive speckle images have been introduced [15], the intrinsic time-resolution of the methods are limited by the hardware constraint of the detector. Even after the many years of technological evolutions, the frame rate of a mega-pixel 2D detector with a large dynamic range (∼16 bit) is still limited to hundreds of milliseconds. More recently, multi-exposure speckle method has provided [16, 17] means to study transient dynamics in various systems by measuring variance of intensity among the pixels of the camera as a function of light exposure durations. Later a more advanced multi-exposure speckle imaging was introduced, in which an improved time-resolution was demonstrated down to tens of microseconds and the choice of the 2D detector became flexible [18].

In this work, we demonstrate an alternative light scattering scheme that allows for a simultaneous measurement of structural and dynamical information by using double pulsed laser beam and a mega-pixel 2D detector. The concept of our proposed method is based on the principles of a split-pulse approach [19] where two-equal intensity pulses are separated in time but propagates along the same path. Here, the time-resolution of the measurement is defined by the time-delay between two laser pulses, and thus allowing to resolve dynamics that are much faster than the response time of the detector. As for an additional advantage for using the 2D detector in such transient speckle measurements, amount of data that are contained in a single image is equivalent to having million photodiodes measuring the scattering signals or collecting it with a single photodiode for over million times, and thus sufficient data statistics can be acquired in a considerably shorter amount of time.

2. Theory

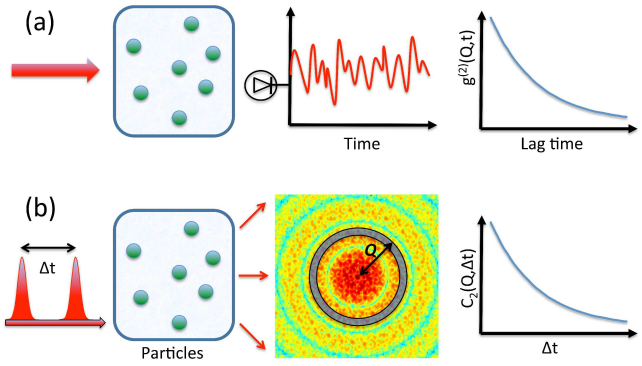

Fig. 1. (a) A dynamical light scattering measures particle motions via intensity correlation function g_2 as a function of lag time while the split-delay approach (b) deduces equivalent information from the evolution of speckle contrast as a function of time-delay Δt between two laser pulses.

#216973 - $15.00 USD Received 14 Jul 2014; revised 14 Aug 2014; accepted 14 Aug 2014; published 28 Aug 2014

Main components of a typical DLS setup consist of a monochromatic and coherent light source such as a laser, a diffractometer and a high-speed point detector (see Fig. 1(a)). Time-dependent fluctuations of scattered photons are measured at a fixed angle that corresponds to a scattering wavevector ($Q = \frac{4\pi n}{\lambda}\sin(\frac{\theta}{2})$), where n, λ and θ are refractive index of the solution, the laser wavelength and the scattering angle respectively. Given that the coherence volume is comparable or greater than the scattering volume, the dynamical information of the particles can be derived from the intensity correlation function

$$g^{(2)}(Q,\tau) = \frac{\langle I(t)I(t+\tau)\rangle}{\langle I(t)\rangle^2}, \tag{1}$$

where τ is the lag time, *I(t)* is the intensity at time t. According to the Siegert relation, the first order autocorrelation function $g^{(1)}(Q,\tau)$ can be deduced as follows

$$g^{(2)}(Q,\tau) = 1 + \beta_o^2 |g^{(1)}(Q,\tau)|^2 \tag{2}$$

where β_o is the contrast scaling factor that depends on the quality of optics and alignment in the experimental setup. For a monodisperse particle system, $g^{(1)}(Q,\tau)$ can be treated as an exponential decay function $g^{(1)}(Q,\tau) = \exp(-\gamma\tau)$ where γ is the decay rate, from which the translational diffusion coefficient D of the particles can be calculated via a relation $\gamma = Q^2 D$ [20]. However in order to achieve a sufficient statistical accuracy, a time-averaged data acquisition is required at a fixed Q, which prohibits simultaneous measurement of overall intensity structures.

In the split-pulse approach (see Fig. 1(b)) however, two equal intensity pulses are delayed with respect to each other by Δt and then incident on the sample. Subsequently the scattered speckle patterns, which is essentially a sum of two independent speckle events, $I(t)$ and $I(t+\Delta t)$, are imprinted on an area detector. More specifically, given that the temporal width and separation between the pulses can be accurately controlled, the time-resolution of the scheme becomes independent of number of pixels or the frame rate of the detector. When the scattering pattern is recorded by the detector, the normalized variance of intensity distribution at a wavevector Q can be evaluated as

$$c_2(\Delta t) = \frac{\langle S^2(\Delta t)\rangle - \langle S(\Delta t)\rangle^2}{\langle S(\Delta t)\rangle^2}, \tag{3}$$

$\langle S^2(\Delta t)\rangle$ is given as

$$\langle S^2(\Delta t)\rangle = \langle [I(t) + I(t+\Delta t)][I(t) + I(t+\Delta t)]\rangle, \tag{4}$$

and the squared mean intensity is

$$\langle S(\Delta t)\rangle^2 = \langle I(t) + I(t+\Delta t)\rangle^2, \tag{5}$$

where $S(\Delta t)$ is the intensity measured by the detector pixels. Here we note that speckle contrast β is given by the variance and the mean intensity of the speckle pattern via $\beta = \sqrt{c_2}$. Taking an effect of shot noise (α), Gutt et al., has shown that $c_2(\Delta t)$ is equivalent to the intensity correlation function $g^{(2)}(\tau)$ and thus allowing a direct measurement of an intermediate scattering function via following relation [19]

$$c_2(Q,\Delta t) = \frac{\beta_o^2}{2}(1 + |\exp(-\gamma(Q)\Delta t)|^2) + \alpha. \tag{6}$$

#216973 - $15.00 USD Received 14 Jul 2014; revised 14 Aug 2014; accepted 14 Aug 2014; published 28 Aug 2014

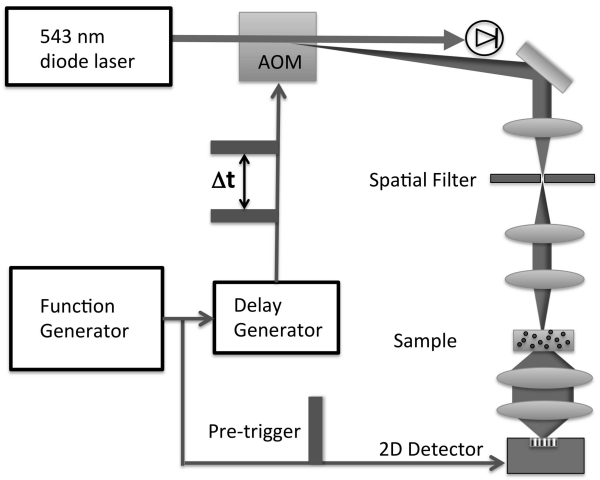

Fig. 2. The schematic of experimental setup consists of a diode laser with a center wavelength of 532 nm, AOM, an electronic waveform generator and a delay generator. Pulsed laser beams are delivered to the colloidal samples and the scattering signals are imaged onto a 2D detector after the image-relaying optics

3. Experimental setup

The overall experimental setup is illustrated in Fig. 2. The optical layout comprises series of elements for delivering the coherent monochromatic pulses to the sample and relaying scattering signals onto a 2D detector. The light source is a single frequency diode-pumped solid-state DPSS laser (Cobolt Samba) operating at a center wavelength of 532 nm. We placed a half-wave plate and a polarizer at the output to control the beam intensity. The CW laser beam is initially collimated and then directed to the AOM. We then focused the diffracted output from the AOM via a 10 cm focal length bi-convex lens and send it through 50 μm pin-hole to filter unwanted aberrations in the beam that are caused by the upstream optics. Finally the filtered beam is re-collimated and focused after two bi-convex lenses (focal length of 20 cm each) before reaching the sample cell that is made of research grade quartz glass. Here we note that the incident light is vertically polarised. Scattered signals from the sample are collected by our image-relay setup, which consists of two bi-convex lenses whose focal length and diameters are 10 cm and 15 cm respectively. The scattering angles that are accessible in our setup ranges from 4° to 18° corresponding to wavevectors between 1 μm^{-1} and 5 μm^{-1}. The minimal angle is limited by the size of the optical beam block that prevents the transmitted main beam from reaching the detector. However, we expect that the current limitation of the angular acceptance in the image-relay scheme can be overcome with a use of higher quality aspherical lenses to minimize the spherical aberration or by implementing a more elaborate optical layout [21], which is beyond the scope of this study. Presently, higher wavevectors beyond the accessibility provided in our optical setup can be reached by rotating the detector about the sample cell position. As for the 2D detector, we used a 16 bit CMOS (Andor Neo) camera with 2560×2160 pixels with each pixel size of 6.5×6.5 μm^2. While utilizing the full detection area, the maximum frame rate of the camera is limited to 10 frames per second. During the data collection, an arbitrary waveform generator (Tektronix AFG 3022B) sends out a master trigger to a delay generator (Stanford Research Systems 553), which subsequently redistributes two square pulses with widths and time-delays of our choice. The CW laser beam is now double-pulsed after the AOM with its

#216973 - $15.00 USD Received 14 Jul 2014; revised 14 Aug 2014; accepted 14 Aug 2014; published 28 Aug 2014

modulation input sent from the delay generator. The CMOS camera is pre-triggered by a TTL signal sent from the waveform generator to capture scattering intensities from the two pulses within its exposure duration.

4. Result and analysis

4.1. Two-pulse speckle correlation as a function of Q

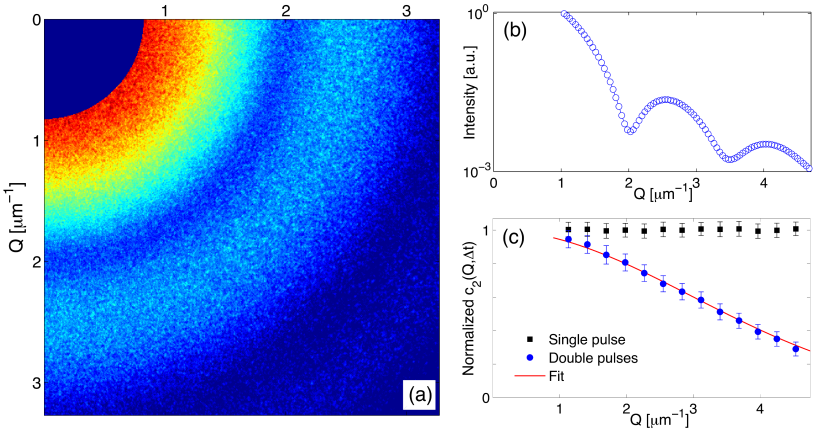

Fig. 3. (a) A single frame image of a double-pulse based 4.5 μm polystyrene particle diffraction pattern taken with Δt = 300 ms shows concentric rings that are the signature of the diffraction pattern from spherical particles with a well defined diameter. A false color representation in the figure corresponds to the intensity distribution of the scattered light from the sample recorded on the 2D detector where the color gradient from red to blue indicates reduction in collected light intensities. (b) Scattering intensity as a function of the momentum transfer Q. (c) The speckle contrasts as a function of Q for single pulse (black square) and two-pulse measurements (blue circle) are compared. The numerical fit of the two-pulse data using Eq. (6) (solid red) can be used to calculate the diffusion coefficient of the particles.

In connection to Eq. (6), we present an alternative approach to measure the transient dynamics of the particles from a single image instead of measuring c_2 as a function of time-delays. The reduction of the speckle contrast occurs when the dynamics in the sample is fast as compared to the time-delays between the two pulses. According to this principle, we can choose a specific time-delay, such that the c_2 measured at different Q covered on our detector area carry different decay rates. Subsequently we can numerically solve for γ in Eq. (6) by using different Q values as a variable and a fixed value for Δt as follows:

$$\gamma(Q) = -\frac{1}{2\Delta t} ln(\frac{2}{\beta_o^2}(c_2(Q,\Delta t) - \alpha) - 1). \tag{7}$$

In this initial split-pulse correlation experiment, we used a diluted suspension of polystyrene spheres (Polysciences, Inc. 17135-5) with a mean diameter of 4.518 $\pm$ 0.152 μm. The sample was prepared at a volume fraction of 3×10^{-5} and placed in a 1 mm thick quartz glass cell and kept at an ambient temperature of 20$\pm$0.1°. While the density of the prepared particles closely matches the water solution within 4% to minimize the effect of the sedimentation, we note that the two-pulse approach is insensitive to a long term drift such as sedimentation or

#216973 - $15.00 USD Received 14 Jul 2014; revised 14 Aug 2014; accepted 14 Aug 2014; published 28 Aug 2014

power drift of the laser as long as those effects are slow as compared to the time-delay between two pulses. Relatively large polystyrene particles were used such that several form factor rings can be captured on our imaging system, in which 1500×1500 pixels were used to resolve the scattering pattern. For this measurement, a time-delay of Δt = 300 ms was chosen such that the speckle patterns at high Q region in the image would be primarily sensitive to the particle motions. Here, 100 frames are taken to achieve sufficient data statistics.

Figures 3(a) and 3(b) show the grainy speckle features appearing on the concentric rings that are the signature of the diffraction pattern from spherical particles with a well defined diameter and azimuthally averaged scattering intensity as a function of the momentum transfer Q respectively. Here in order to evaluate the speckle contrasts as a function of Q, the pixel elements centered about the optical axis (Q = 0) were used for the speckle calculation where we selected regions of interest consisting of an annulus of radius Q and width of 20 pixels (corresponding to $\Delta Q \approx 0.07\ \mu\mathrm{m}^{-1}$). The speckle contrasts are calculated from the normalized standard deviation of the intensity fluctuation $\beta = \sigma_I/\langle I\rangle$. We note that, given sufficient photon intensities, the intensity probability distribution function $P(I)$ of these fully developed speckle patterns follows the Gamma density distribution function [22, 23]

$$P_M(i) = M^M(i/ < i >)^{M-1}e^{-Mi/<i>}/(\Gamma(M) < i >), \tag{8}$$

where i is intensity measured on a detector pixel, $< i >$ is the mean intensity, M is the number of speckle modes and Γ is the gamma function. The speckle contrast β is connected to the number of speckle mode via the relation $\beta = 1/\sqrt{M}$. Finally the normalized variance c_2 is obtained via $c_2 = \beta^2$.

When a single laser pulse with a duration of 10 μs was used to collect the image, no reduction in c_2 was observed, which implies no significant dynamics taking place at this time and length scales (See Fig. 3(c)). However when two pulses with the time-delay of 300 ms were used to collect the scattering image, clear reductions in c_2 are observed from Q = 1.0 $\sim$ 4.0 $\mu\mathrm{m}^{-1}$. Numerical fitting of Eq. (6) to the data set via chi-square minimization [24] yields a diffusion coefficient $D = 9.65\times10^{-14}\ \mathrm{m}^2/s$ with a standard error of $0.17\times10^{-14}\ \mathrm{m}^2/s$. This value is consistent with the expected diffusion of coefficient of 4.5 μm particles in water, which is $9.75\times10^{-14}\ \mathrm{m}^2/s$. Subsequently the mean particle diameter can be confirmed via the Stoke-Einstein relation $D = k_BT/6\pi\eta r_p$ where k_B, T, η, and r_p are Boltzmann's constant, absolute temperature, solution viscosity and the radius of the spherical particles respectively. This alternate approach to obtain speckle dynamics while monitoring the intensity structure of the scattering pattern may be very useful when studying continuously changing system without sacrificing the time-resolution due to relatively slow frame rate of the 2D detector.

4.2. Two-pulse speckle correlation as a function of Δt

In order to demonstrate a microsecond time-resolution measurement with our large area 2D detector, the polystyrene particles (Polyscience, Inc 08691-10) with a diameter of 50±4 nm were prepared. This measurement was made at a considerably larger scattering angle of 34° corresponding to a wavevector of Q = 9.2 $\mu\mathrm{m}^{-1}$ at an ambient temperature of 23±0.1°. This wide angle scattering measurement was achieved by rotating the detector about the sample position and changing the laser pulse widths to 1 μs. In this part of the experiment, the image-relaying optics were removed and the sample to detector distance was adjusted to 17 cm. Here 500×500 pixels were chosen as a region of interest to cover $\Delta Q \approx 0.2\ \mu\mathrm{m}^{-1}$. Finally the speckle contrasts are calculated at different time-delays ranging from 0.1 μs to 10 ms. Unlike the conventional DLS approach, this method does not require having measurement made at fixed time intervals. And thus, one can use fine time steps for capturing fast dynamics while more coarse steps can be employed for measuring slower dynamics to reduce data acquisition

#216973 - $15.00 USD Received 14 Jul 2014; revised 14 Aug 2014; accepted 14 Aug 2014; published 28 Aug 2014

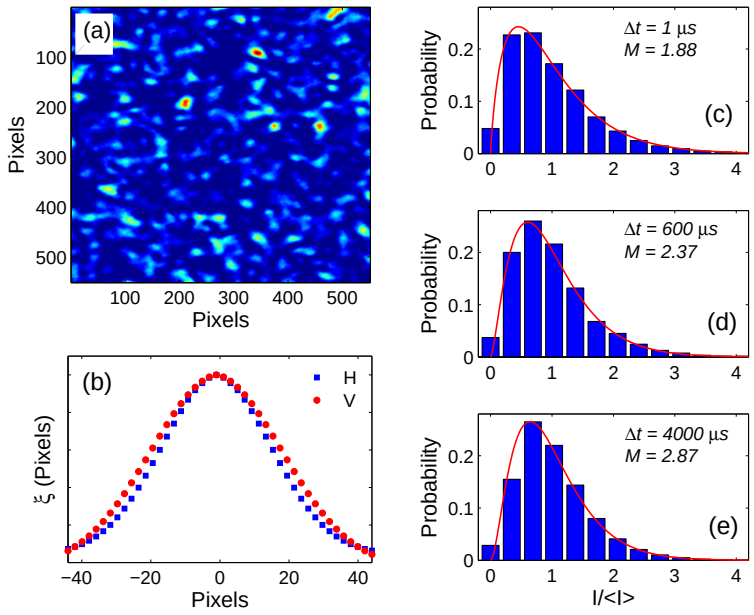

Fig. 4. (a) A typical speckle patterns measured from 50 nm polystyrene nano particles measured at 34°. (b) Spatial intensity autocorrelation of the image yields the symmetric speckle width along two orthogonal directions. H and V denote horizontal and vertical directions along the 2D detector respectavely. (c)-(e) Intensity distribution function from the double-pulsed speckle patterns measured at different delay-times.

time. In this measurement, 100 images were taken at each time-delay.

Figure 4(a) shows a snap shot of a typical speckle pattern recorded on the detector. Pronounced grainy structures in the image reflect the spatial arrangements of the colloidal particles, where the spatial intensity correlation function $\xi(R) = \langle I(r+R)I(r)\rangle/\langle I(r)\rangle^2$ yields the size of the speckle width. As shown in Fig. 4(b), equivalent speckle size along two perpendicular directions ($\sim$40 pixels) implies a symmetric beam profile impinging on the sample. Histogrammed data sets in Figs. 4(c)–4(e) show the normalized intensity distribution measured by the detector pixels within the region of interest. Red lines show the fitted results of Eq. (8) to the experimental data at subsequent time-delays of Δt = 1, 600, and 4000 μs respectively. Initially at Δt=1 μs, since the correlation time of the particle movements is sufficiently longer than the time-delay, the speckle contrast of 0.73 from the sum of the two pulses is equal to that of a static image. On the other hand, when Δt becomes longer than the correlation time, reductions (0.65 and 0.59 for each time-delay of 600 μs and 4000 μs respectively) of the speckle contrasts can be observed. Figure 5 shows the evolution of c_2 as a function of Δt. The initial plateau in the correlation plot confirms that the particle dynamics at this length scale does not change within the pulse-width of 1 μs. The correlation curve however shows a rapid decay from approximately 10^2 μs to 10^4 μs time interval. Here, fitting Eq. (6) to the experimental data via chi-square minimisation yields $\gamma = 828.52$ s^{-1} with a standard error of 71 s^{-1} and the translational diffusion coefficient of $(9.79\pm0.84)\times10^{-12}$ m$^2/s$. The particle diameter, which is calculated by using the Stoke-Einstein relation, yields 50.07$\pm$4.29 nm that is consistent with

#216973 - $15.00 USD Received 14 Jul 2014; revised 14 Aug 2014; accepted 14 Aug 2014; published 28 Aug 2014

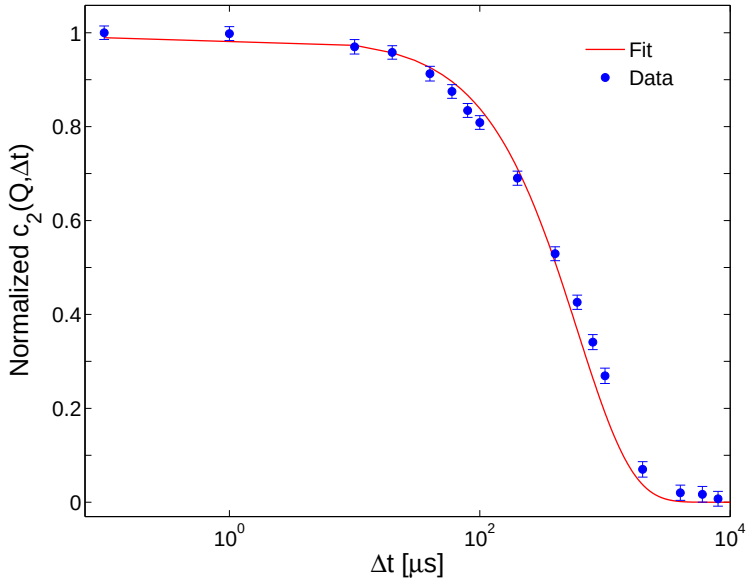

Fig. 5. Speckle contrast correlation function $c_2(\Delta\tau)$ measured from speckle patterns of 50 nm polystyrene particles at a diffraction angle of 34°.

the manufacturer′s specification.

Figure 6 shows a normalised speckle contrast correlation values measured at $\Delta t = 1\mu$s as a function of the number of images averaged N where the error bars are given by the standard deviation of the mean. In this experimental demonstration, since the correlation value stably converges at around N = 100, we have used the speckle contrast correlation values that are obtained by averaging the results from each of the 100 images. However as can be seen in Fig. 6, the values are relatively accurate even at N = 10 or less. In practice, we can drastically reduce the acquisition time by a factor of 10 or more by cumulating less number of images.

5. Conclusion

We have demonstrated an alternate light scattering method that enables simultaneous measurements of high-speed dynamics and structural information of colloidal particles via the two-pulse speckle contrast correlation. In this new approach, a direct ensemble averaging can be achieved without needing for an extensive time-averaging or at the expanse of time-resolution that had been previously limited by slow frame rates of the 2D megapixel detectors. Here, we note that the form of $g^{(1)}$ used in our present work assumes that dynamics of colloidal particles are independent and the measurements were performed in the single-scattering regime, which is appropriate for the diluted colloidal systems. However our method is not just limited to the diluted colloidal systems. Also more concentrated solutions (with considerable inter-particle correlations) or particle dynamics under flow conditions can still be studied, in which case other forms of $g^{(1)}$ function [4, 16, 25] can be employed. We also note that the ultimate time-resolution of our current setup is limited by the response time of the AOM, which is $\sim$1 μs. This temporal limitation can be possibly overcome by using a femtosecond laser source such as Ti:Sapphire laser systems, which will reduce the pulse durations down to tens of femtoseconds.

#216973 - $15.00 USD Received 14 Jul 2014; revised 14 Aug 2014; accepted 14 Aug 2014; published 28 Aug 2014

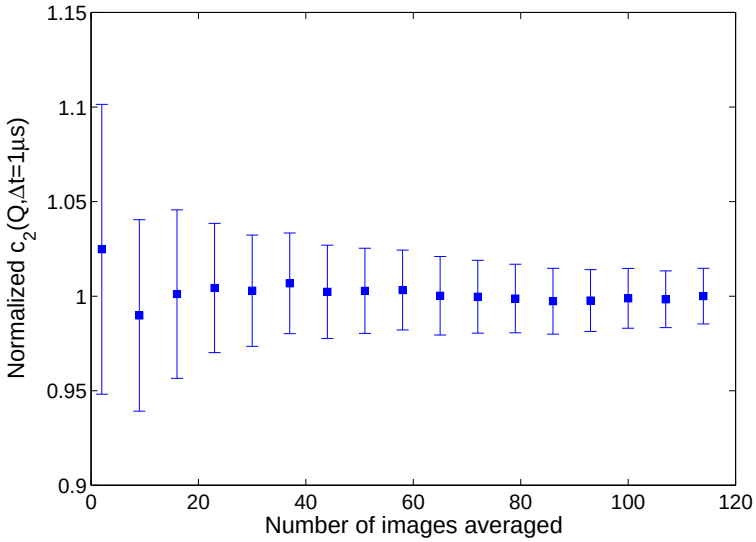

Fig. 6. Normalized speckle contrast correlation values as a function of number of images averaged.

Ultimately, our work presents an effective way to probe a wide range of system sizes from micro-to-nanometers and times-scales down to microseconds. The successful demonstration of this method provides a very promising prospect to perform speckle correlation experiments at the x-ray free electron laser facilities [26, 27] that have been developed to study ultrafast dynamics at atomic time and length scales.

Acknowledgments

This research was supported by the Converging Research Center Program through the Ministry of Science, ICT and Future Planning, Korea (NRF-2014M3C1A8048818, NRF-2014M1A7A1A01030128). C.G. acknowledges financial support from the BMBF under contract No. 05K2013-605.

#216973 - $15.00 USD Received 14 Jul 2014; revised 14 Aug 2014; accepted 14 Aug 2014; published 28 Aug 2014